High Carbon Use Efficiency in Soil Microbial Communities Is Related to Balanced Growth, not Storage Compound Synthesis

Paul Dijkstra[1,2], Elena Salpas[1], Dawson Fairbanks[1,3], Erin B. Miller[1], Shannon B. Hagerty[1,4], Kees Jan van Groenigen[1,2], Bruce A. Hungate[1,2], Jane C. Marks[1,2], George W. Koch[1,2] and Egbert Schwartz[1]

[1]Department of Biological Sciences, Northern Arizona University, PO Box 5640, Flagstaff, AZ, U.S.A.

[2]Center for Ecosystem Science and Society, Northern Arizona University, PO Box 5640, Flagstaff, AZ, U.S.A.

[3]Current address: Dept. Soil, Water and Environmental Sciences, University of Arizona, PO Box 210038, Tucson, AZ, U.S.A.

[4]Current address: Dept. of Ecology, Evolution, and Marine Biology, University of California, Santa Barbara, PO Box 9620, Santa Barbara, CA, U.S.A.

Corresponding author: Paul Dijkstra: paul.dijkstra@nau.edu, tel 928-523-0432 /928-707-4486, fax 928-523-7500, PO Box 5640, Flagstaff AZ, USA.

Running title: Carbon Use Efficiency in Microbial Communities

Keywords: fluxomics/ glycogen / metabolic model /polyhydroxybutyrate /position-specific labeling/ tri-palmitoyl-glycerol

ABSTRACT

The efficiency with which microbes use substrate (Carbon Use Efficiency or CUE) to make new microbial biomass is an important variable in soil and ecosystem C cycling models. It is generally assumed that CUE of microbial activity in soils is low, however measured values vary widely. It is hypothesized that high values of CUE observed in especially short-term incubations reflect the build-up of storage compounds in response to a sudden increase in substrate availability and are therefore not representative of CUE of microbial activity in unamended soil.

To test this hypothesis, we measured the $^{13}CO_2$ release from six position-specific ^{13}C-labeled glucose isotopomers in ponderosa pine and piñon-juniper soil. We compared this position-specific CO_2 production pattern with patterns expected for 1) balanced microbial growth (synthesis of all compounds needed to build new microbial cells) at a low, medium, or high CUE, and 2) synthesis of storage compounds (glycogen, tri-palmitoyl-glycerol, and polyhydroxybutyrate).

Results of this study show that synthesis of storage compounds is not responsible for the observed high CUE. Instead, it is the position-specific CO_2 production expected for balanced growth and high CUE that best matches the observed CO_2 production pattern in these two soils. Comparison with published studies suggests that the amount of glucose added in this study is too low and the duration of the experiment too short to affect microbial metabolism. We conclude that the hypothesis of high CUE in undisturbed soil remains viable and worthy of further testing.

1. Introduction

Heterotrophic microbes use organic carbon (C) compounds to synthesize cellular compounds while releasing some substrate-C as CO_2. Which compounds are synthesized depends on the physiology of the cells (active growth and division, survival when substrate availability is low, dormancy). It is currently not possible to determine directly the compounds that are produced. It seems plausible that the microbial community consists of cells in all possible physiological states at any time, unless there are synchronizing events, such as a simultaneous depletion of substrate in all soil niches or a sudden increase in substrate availability. The C Use Efficiency (CUE; biomass-C synthesized per substrate-C consumed; mol C / mol C) of the soil microbial community is an important ecosystem variable that influences what proportion of organic C utilized is released to the atmosphere as CO_2 or potentially remains in the soil as organic matter in living cells or dead soil organic matter (Billings & Ballantyne, 2013; Bradford, 2013; Hagerty et al., 2014). Indirectly, CUE also determines whether nutrients such as nitrogen (N) or phosphate are immobilized or mineralized (Manzoni et al., 2012; Sinsabaugh et al., 2013). Consequently, an improved understanding of CUE is important for soil C and N cycling models (Allison et al., 2010; Hagerty et al., 2014; Li et al., 2014; Manzoni et al., 2012; Wieder et al., 2013). The CUE is a function of the cellular demand for energy and biosynthesis, and therefore a function of the physiological state and compounds that are being produced. When only energy is required (such as for cell maintenance), CUE is close or equal to zero (Amthor 2000; Chapman & Gray, 1986).

Because of low C availability in soil and the supposedly recalcitrant nature of soil organic matter, the CUE of the microbial community is often assumed to be low (Anderson & Domsch, 2010; Manzoni et al., 2012; Reischke et al., 2015; Sinsabaugh et al., 2013). The limited substrate available is used to satisfy energy demands for cell maintenance with little left for growth. However, many studies find high values of CUE (0.6 and higher; e.g., Brant et al., 2006; Dijkstra et al., 2011a,b; Frey et al., 2013; van Groenigen et al., 2013; Hagerty et al., 2014; Steinweg et al., 2008; Thiet et al., 2006; Tucker et al., 2013; Ziegler et

al., 2005). The average CUE observed in soil is 0.55 (Manzoni et al., 2012; Sinsabaugh et al., 2013). This value is remarkably close to the average maximum value of CUE observed in pure culture studies (~0.6; Blagodatskaya et al., 2014; Roels, 1980; Sinsabaugh et al., 2013), but below the theoretical thermodynamic maximal CUE of growth on glucose (0.88 – 1.0; Gommers et al., 1988; Heijnen, 2010; Heijnen & van Dijken, 1992; Manzoni et al., 2012; Roels, 1980; Xiao & van Briesen, 2006). The average CUE for soil is much higher than that found in aquatic ecosystems (~0.3; Hobbie & Hobbie, 2013; Manzoni et al., 2012; Sinsabaugh et al., 2013). This large discrepancy in CUE raised concerns (Hobbie & Hobbie 2013; Sinsabaugh et al., 2013), prompting a critical evaluation of methods used to determine community CUE (Sinsabaugh et al., 2013).

The measurement of CUE often involves adding (^{13}C-enriched) substrates. It is suggested that high substrate additions alter CUE, either increasing (van Groenigen et al., 2013; Sinsabaugh et al., 2013) or decreasing it (van Groenigen et al., 2013; Russell, 2002). Specifically for short-term experiments, it is hypothesized that high CUE values may not represent microbial balanced growth (that is, the synthesis of all compounds to build new cells), but instead may be the result of rapid uptake of substrate followed by synthesis of storage compounds (Blagodatskaya et al., 2014; Hill et al., 2008; Nguyen & Guckert, 2001; Reischke et al., 2014, 2015; Sinsabaugh et al., 2013). Although this still represents an increase in biomass, for a sound understanding of C cycling in soil ecosystems, it is important to distinguish between CUE during long-term microbial activity and that where microbes temporarily allocate C to storage synthesis associated with a sudden and temporary increase in substrate availability (Sinsabaugh et al., 2013). Microbial cells can store substrate as starch, glycogen, trehalose, extracellular polysaccharides (Wilson et al., 2010), polyhydroxyalkanoates and storage lipids (Lu et al., 2009; Olsson & Johansen, 2000). However, measurements of storage synthesis in soil have not been made.

In this study we evaluate four mutually exclusive hypotheses: 1) the microbial community uses substrate for maintenance only (CUE = 0); 2) the microbial community exhibits balanced growth but an

overall low CUE (CUE = 0.3 as suggested by Sinsabaugh et al., 2013), 3) the microbial community exhibits a high CUE but "unbalanced" growth where biosynthesis is limited to storage compound production (glycogen, lipids, or polyhydroxybutyrate), and 4) the microbial community exhibits balanced growth at high CUE (0.6; close to the maximal CUE in pure culture studies).

We conducted an incubation experiment with six position-specific ^{13}C-labeled glucose isotopomers and two soils from northern Arizona, USA. We compared the observed pattern of position-specific CO_2 production with patterns predicted for balanced microbial growth at varying CUE (CUE = 0, 0.3, or 0.6) and storage synthesis (glycogen, tri-palmitoyl-glycerol - TPG - and polyhydroxybutyrate - PHB). By comparing our experimental methods and results with published studies of responses of microbial growth to substrate addition, we test a fifth hypothesis that the increase in substrate availability changed the CUE of the microbial community. We show that the observed position-specific CO_2 production resembles patterns expected for balanced growth at high CUE, does not match CO_2 production patterns of any combination of low or medium CUE and storage compound synthesis. According to current published research results, these results were not affected by the change in substrate availability.

2. Materials and methods

2.1 Experimental procedures

We collected soil (0-10 cm depth) from two locations along the C. Hart Merriam Elevation Gradient (www.nau.edu/Ecoss/) near Flagstaff, Arizona. The highest site (2340 m elevation, mean annual temperature (MAT) 8°C, mean annual precipitation (MAP) 660 mm) was a small open area in a ponderosa pine (*Pinus ponderosa*) stand covered with blue grama (*Bouteloua gracilis*). Soil was a Mollic Eutroboralf (C content 1.5%, N content 0.11%; Dijkstra et al., 2006). The second site (2020 m elevation, MAT 10°C, MAP 380 mm) was an intercanopy space in a piñon-juniper stand (*Pinus edulis*, *Juniperus monosperma*) also covered with blue grama grass. Soil type was a Calcic Haplustand (C content 1.7%, N content 0.16%; Dijkstra et al., 2006). Soil was sieved (2 mm mesh) and stored at 4°C until used in the fall of 2012.

We weighed 40 g of sieved soil into a specimen cup and placed in a Mason jar (473 ml) equipped with an airtight lid and septum (n = 4). Soil moisture content was adjusted to field capacity (0.272 and 0.300 g water g^{-1} soil dry weight for respectively ponderosa pine and piñon-juniper soil) and incubated overnight in the dark at room temperature (21°C). The next morning, jars were opened, headspace atmosphere was replaced with lab air, and, after closing the jar, 10 ml of pure CO_2 was added to the headspace. This addition of pure CO_2 was needed to have enough CO_2 in 10 ml headspace gas samples for the Picarro 2101-*i* CO_2 isotope spectrometer (Picarro Inc, Sunnyvale, CA) to measure isotope ratios within the calibrated range of concentrations (Dijkstra et al., 2011a). After 30 min and before glucose isotopologue addition, a 10 ml headspace gas sample was taken (time zero).

We used glucose (^{13}C-labeled in C_1, C_2, C_3, C_4, C_5, C_6 and uniformly (U) labeled) as the metabolic tracer (99 atom fraction %; Cambridge Isotope Laboratories, Andover, Massachusetts). Two ml of a 1.79 mM glucose isotopomer solution was added to each specimen cup (0.536 µmol glucose-C g^{-1} soil; n = 4). Because of the large number of isotopologues, replicates, each consisting of seven glucose isotopologue

incubations, were done on successive days. Ten ml headspace gas samples were taken 20, 40, and 60 min after tracer addition and analyzed for isotope composition with the Picarro CO_2 isotope analyzer. The isotope composition of headspace CO_2 was expressed as atom fraction excess (%; Coplen, 2011) and plotted against time. We determined the slope of atom fraction excess (calculated as the difference between the atom fraction at t=1 and the atom fraction at t=0) for the period that the CO_2 production rate was constant (40 min, Fig. 3a) and calculated the ratio of position-specific CO_2 production rates as follows:

$$\frac{Cx}{CU} = \frac{^{13}CO_2\ production\ from\ x{-}^{13}C\ glucose}{^{13}CO_2\ production\ from\ U{-}^{13}C\ glucose} \quad (1)$$

where x stands for each of the six C-atoms in glucose and U for the uniformly labeled glucose isotopologue. Ratios were calculated for each replicate.

2.2 Modeling

We used the metabolic model of the central C metabolic network (CCMN) as described in Dijkstra et al. (2011a) with small modifications (Fig. 1). In short, this model included glycolysis, pentose phosphate pathway (PP-pathway), TCA cycle, pyruvate carboxylase as the anaplerotic reaction, and eight precursor-consuming biosynthesis reactions. The model assumed that glucose is the only substrate for cell metabolism. The model included consumption of CCMN intermediates for biomass synthesis. The model did not make any assumptions about microbial growth rates or CUE, but assumed that all biomass synthesis reactions consumed precursors in constant proportion (in other words a constant chemical composition of the cell). The proportional precursor demand (demand for precursors to enable balanced growth) was br1 : br2 : br3 : br4 : br5 : br6 : br7 : br8 = 1 : 0.32 : 9.29 : 11.63 : 13.20 : 5.01 : 7.44 : 4.89 representative of Gram-negative bacteria, estimated from pure culture studies (Dijkstra et al., 2011a). We compared the position-specific CO_2 fluxes for Gram-negative bacteria with CO_2 fluxes for Gram-positive bacteria and fungi which have slightly different precursor demands and chemical

153 composition (see below; Dijkstra et al., 2011a). The model calculated the fate of each C atom in glucose
154 and the probability that it is released as CO_2 by pyruvate dehydrogenase, isocitrate dehydrogenase, α-
155 ketoglutarate dehydrogenase or phosphogluconate dehydrogenase. Carbon use efficiency of the
156 microbial community was calculated from the model as

157 $$CUE = 1 - \frac{\sum(r5,r6,r7,r9)}{6 \times r1} \quad \text{(eq. 2).}$$

158 with *r5*, *r6*, *r7*, *r9* as the rate of the CO_2-releasing reactions r5, r6, r7, and r9 respectively, and *r1* as the
159 rate of substrate uptake r1 (Fig. 1). For further details, see Dijkstra et al. (2011a, b), van Groenigen et al.
160 (2013), and supplemental information with Hagerty et al. (2014).

161 Molar flux rates of the CCMN processes (relative to glucose uptake) were estimated by matching
162 observed and modeled patterns of position-specific CO_2 production. In the previous version of this
163 model, isotopologue pairs of glucose and pyruvate were used. In this study, we solved the model using
164 the six isotopologue ratios (eq. 1) of glucose. A model solution was calculated by minimizing the sum of
165 squares (SS) of the difference between observed and predicted ratios for the six glucose isotopomers by
166 altering the reaction rates *r9* and *br1* (Fig. 1) using the Excel linear programming tool Solver. A local
167 minimum of SS was sometimes observed when model calculations were initiated with *r9* and *br1* equal
168 to zero. For these solutions, R^2 was low and the regression had a negative slope. These results were
169 avoided when initiating the Solver procedure with *r9* and *br1* greater than 0.5.
170
171 *2.3 Calculation of position-specific CO_2 production for balanced growth with low, medium, and high CUE*
172 The metabolic model (Fig. 1) is typically used to find the flux rates through the CCMN processes
173 and CUE by matching modeled glucose (and pyruvate) isotopomer ratios to ratios observed in soil.
174 However, the model can also be used in reverse to calculate glucose position-specific CO_2 production
175 rates (or isotopomer ratios) for hypothetical situations. We used the model to calculate the hypothetical
176 position-specific CO_2 production rates for CUE equal to 0 (*i.e.*, only synthesis of ATP for maintenance

177 processes), CUE equal to 0.3 (*i.e.*, most likely CUE in soil ecosystems as proposed by Sinsabaugh et al.,
178 2013), and CUE equal to 0.6 (*i.e.*, CUE similar to the maximum observed in pure culture studies). For CUE
179 equal to 0.3 or 0.6, position-specific CO_2 production was calculated assuming balanced microbial growth
180 (synthesis of all compounds to build new microbial biomass plus energy for maintenance). Because the
181 position-specific CO_2 production patterns were strongly influenced by the activity of the PP-pathway, we
182 modeled CO_2 production patterns for minimal and maximal PP-pathway activity for Gram-negative
183 bacteria separately (see above for proportional precursor demand). For maximal PP-pathway activity,
184 we set the value of *r2* (Fig. 1) to zero, so that all flux was directed via the PP-pathway. Substrate was
185 returned to the glycolysis as fructose-6P and glyceraldehyde-3P. For minimal PP-pathway activity, the
186 flux of substrate into the PP-pathway was set to that required for growth (*r9* = *br8*), but no substrate
187 was cycled through the PP-pathway back into glycolysis. For these two situations, *br1* was then manually
188 changed until the calculated value of CUE equaled the desired value (0, 0.3, or 0.6).
189 Calculation of position-specific CO_2 production patterns for the situation of "unbalanced"
190 growth (production of reserve compounds only) is described below. To evaluate the sensitivity of
191 position-specific CO_2 production rates for variation in proportional precursor demand, we compared the
192 position-specific CO_2 production for the situation of balanced growth, CUE equal to 0.6, and minimal and
193 maximal activity of the PP-pathway for Gram-negative bacteria (see above), Gram-positive bacteria (1 :
194 0.47 : 5.01 : 5.53 : 6.28 : 3.27 : 4.28 : 2.54) and fungi (1 : 0.18 : 1.30 : 1.45 : 1.72 : 1.04 : 1.08 : 0.60).
195
196 *2.4 Calculation of position-specific CO_2 production for storage compound synthesis*
197 We also calculated the CUE and position-specific CO_2 production of cells that synthesize
198 glycogen (as an example of carbohydrate storage), PHB (an example of polyhydroxyalkanoates), and TPG
199 (an example of lipid storage) by taking into account the amount of ATP and precursors needed for

200 biosynthesis. Information on synthesis pathway stoichiometry and energy demand was obtained from
201 MetaCyc.org (Caspi et al., 2014) and is detailed in sections 2.4.1-2.4.3.

202 We manually calculated the position-specific CO_2 production rates for synthesis of glycogen,
203 TPG, and PHB, again for minimal (all C flows via glycolysis) and maximal activity of the PP-pathway (all C
204 flows via the PP-pathway). Glycogen synthesis included glucose uptake, phosphorylation, and
205 polymerization into glycogen with ATP as the energy donor. ATP was provided by the complete
206 oxidation of a small fraction of glucose to CO_2. Tri-palmitoyl-glycerol was synthesized with acetyl-CoA as
207 the precursor for the fatty acids and dihydroxyacetone-P as the precursor for the glycerol backbone. The
208 ATP needed for this process was produced during the formation of acetyl-CoA via glycolysis and PP-
209 pathway. The extra energy for desaturation of fatty acids came from complete oxidation of a small
210 amount of glucose when PP-pathway activity was minimal. When PP-pathway activity was maximal,
211 enough ATP was produced for fatty acid production and subsequent desaturation reactions. Synthesis of
212 PHB was accomplished with acetyl-CoA as the only precursor, and all required energy was produced
213 during acetyl-CoA production via glycolysis or PP-pathway.

214 During the synthesis of acetyl-CoA from glucose with minimal PP-pathway activity, C_3 and C_4 of
215 glucose were released as CO_2 by pyruvate dehydrogenase. The remainder (acetyl-CoA) was used for TPG
216 and PHB synthesis (Fig. 2). In this case, C_3 and C_4 of the original glucose molecule were released as CO_2,
217 while C_1, C_2, C_5 and C_6 of glucose were incorporated in acetyl-CoA and ended up in fatty acids or
218 polyhydroxybutyrate.

219 The breakdown of glucose to acetyl-CoA via the PP-pathway was more complex as C_1 of glucose
220 was lost in the first few reactions, and the C_2 and C_3 were rearranged to form fructose-6P and
221 glyceraldehyde-3P (Fig. 2). As part of the PP-pathway, glucose was decarboxylated and the pentose
222 sugars were rearranged to fructose-6P and glyceraldehyde-3P in a ratio of 2 : 1. Fructose-6P then broke

into two molecules glyceraldehyde-3P, which mixed with glyceraldehyde-3P retrieved from the PP-pathway. The next step was the release of CO_2 by pyruvate dehydrogenase to form acetyl-CoA.

For energy production, we assumed that 1 NAD(P)H was equivalent to 2.5 ATP, 1 $FADH_2$ produced 1.5 ATP, and 1 GTP was equal to 1 ATP and were readily exchangeable.

2.4.1 Glycogen

We used glycogen as an example of a storage compound derived from glucose-6P precursors (Wilson et al., 2010). ATP cost for making glycogen included glucose uptake (1 ATP – de Kok et al., 2012), phosphorylation (1 ATP), and transformation to UDP-glucose and polymerization (cost for regenerating UTP is 1 ATP). For high glucose concentrations, glucose can enter microbial cells through facilitated transport, but in this analysis, we assumed low glucose concentrations where proton-coupled symport was more likely (Wilson-O'Brien et al., 2010). Glucose-6P precursor and energy demand for glycogen synthesis was described with the following reaction equation:

$$\text{glucose} + (\text{glucose})_n + 3\ \text{ATP} = (\text{glucose})_{n+1} + 3\ \text{ADP} + 3\ P_i.$$

The ATP needed for uptake and polymerization of 1 mol glucose into glycogen was produced from oxidation of 0.0968 mol glucose.

2.4.2 Tri-Palmitoyl-Glycerol

Storage lipids in fungi and bacteria include triacylglycerides (Alvarez & Steinbuchel, 2002; Kosa & Ragauskas, 2011). Palmitic acid is a common fatty acid in storage lipids in *Glomus* species (Olsson & Johansen, 2000). To make 1 mol TPG, 3 mol palmitic acid and 1 mol glycerol were consumed. To produce 3 mol palmitic acid, twelve mol glucose were metabolized to 24 mol acetyl-CoA while releasing 24 mol CO_2. An additional 0.5 mol glucose was needed to synthesize dihydroxyacetone-P, which was turned into

1 mol glycerol-P and combined with 3 mol palmitic acid to form 1 mol TPG. The stoichiometric reaction equation for the synthesis of TPG via glycolysis (minimal PP-pathway activity) was:

$$12.5\ \text{glucose} + 6\ \text{NAD(P)}^+ + 6\ \text{H}^+ + 16.5\ \text{ATP} = 24\ \text{CO}_2 + 6\ \text{NAD(P)H} + 16.5\ \text{ADP} + 16.5\ \text{P}_i + 1\ \text{TPG}.$$

Assuming that ATP and NAD(P)H were fully interchangeable, this reaction produced 0.5 mol ATP per mol TPG. The introduction of 1.5 double bonds per TPG (Olsson & Johansen, 2000) consumed 1 mol ATP per mol storage lipids. This required an additional 0.032 mol glucose, which was completely oxidized, producing ~0.19 mol CO_2. When substrate was directed via the PP-pathway (maximal PP-pathway activity), the stoichiometric reaction equation for TPG synthesis was:

$$15\ \text{glucose} + 36\ \text{NAD(P)}^+ + 6\ \text{H}^+ + 16.5\ \text{ATP} = 39\ \text{CO}_2 + 36\ \text{NAD(P)H} + 16.5\ \text{ADP} + 16.5\ \text{P}_i + 1\ \text{TPG}.$$

In this case, sufficient ATP was produced to drive desaturation reactions.

2.4.3 Polyhydroxybutyrate

Many bacterial species are able to synthesize polyhydroxyalkanoates as C and energy storage (Lu et al., 2009). Polyhydroxybutyrate is a representative of this class of compounds. For the synthesis of PHB, glucose was taken up by the cell, phosphorylated, and metabolized to acetyl-CoA. Two acetyl-CoA molecules were then combined into 3-hydroxy-butanoyl-CoA and polymerized to PHB, consuming 1 NADPH. The stoichiometric reaction equation for PHB synthesis via glycolysis (minimal PP-pathway activity) was:

$$1\ \text{glucose} + (\text{PHB})_n + 1\ \text{ADP} + 1\ \text{P}_i + 3\ \text{NAD(P)}^+ + 3\ \text{H}^+ = (\text{PHB})_{n+1} + 2\ \text{CO}_2 + 1\ \text{ATP} + 3\ \text{NAD(P)H}.$$

When glucose was directed into the PP-pathway (maximal PP-pathway activity), the equation for PHB synthesis was:

$$6\ \text{glucose} + (\text{PHB})_n + 4\ \text{ADP} + 4\ \text{P}_i + 27\ \text{NAD(P)}^+ + 27\ \text{H}^+ = (\text{PHB})_{n+5} + 16\ \text{CO}_2 + 4\ \text{ATP} + 27\ \text{NAD(P)H}.$$

All ATP required for these reactions was produced during the production of acetyl-CoA.

2.5 Statistical Analysis

One-way analysis of variance was used to evaluate differences between soils. To determine which biochemical scenario (balanced growth with CUE = 0, CUE = 0.3, or CUE = 0.6, synthesis of storage compounds) best explained observed CO_2 production data, we assessed whether the 95% confidence interval of observed isotopomer ratios overlapped with model predictions. Correspondence between observed and predicted position-specific CO_2 production was evaluated using R^2, and closeness of slope and intercept to the expected 1 : 1 line.

277 **3. RESULTS**

278 *3.1 Observed position-specific CO_2 production*

279 We measured the position-specific CO_2 production for glucose in ponderosa pine and piñon-juniper soil.
280 The rate of CO_2 production from glucose isotopomers was constant for 40 minutes (Fig. 3A, results
281 piñon-juniper soil not shown), after which it started to decline as was seen in previous studies (Dijkstra
282 et al., 2011b). There were clear and significant differences in CO_2 production from different C atoms
283 ($P<0.05$): CO_2 production from C_1 was significantly higher than C_4, which was higher than C_2 and C_3, while
284 C_5 and C_6 were the lowest (Fig. 3B). This pattern was the same for both soils. The CUE derived from
285 modeling (following Dijkstra et al., 2011a with slight modifications) was not significantly different
286 between the two soils (0.62 for ponderosa pine soil, 0.61 for piñon-juniper soil).

287

288 *3.2 Modeled position-specific CO_2 production*

289 *3.2.1 Balanced growth and varying CUE*

290 Carbon use efficiency and activity of the PP-pathway had a large influence on the position-
291 specific CO_2 production (Fig. 4). With maximal PP-pathway activity and high CUE, most of the CO_2 was
292 produced from C_1 and C_4; in contrast, when PP-pathway activity was minimal, most CO_2 was produced
293 from C_3 and C_4. With decreasing CUE, these differences became less pronounced. When CUE equaled 0,
294 substrate was used only for synthesis of ATP and NAD(P)H, and all C positions were released as CO_2 at
295 the same rate (ratio of $C_x : C_U = 1 : 6$).

296 The compounds produced to make bacterial or fungal cells differed slightly resulting in small
297 differences in proportional precursor demand between Gram-negative and Gram-positive bacteria and
298 fungi (Dijkstra et al., 2011a). These differences in proportional precursor demand had only a small effect
299 on metabolic flux patterns and CUE (Dijkstra et al., 2011a, b; van Groenigen et al., 2013). This was also
300 true for the position-specific CO_2 production (Fig. 5). For this reason, the results presented for Gram-

301 negative bacteria were considered representative for any combination of fungi, Gram-positive and
302 Gram-negative bacteria.
303
304 *3.2.2 Storage compound synthesis*
305 The CUE of storage compound synthesis was high (Table 1) although dependent on the form of
306 storage (glycogen > TPG ≈ PHB). For TPG and PHB, the CUE was reduced when PP-pathway activity was
307 high.
308 Complete oxidation of glucose to CO_2 was needed to provide the ATP for glycogen synthesis.
309 This resulted in a position-specific CO_2 production that was equal for all C atoms (Table 2), similar to the
310 situation with only maintenance energy (Fig. 4). The ATP required for TPG synthesis was produced
311 during the breakdown of glucose to acetyl-CoA. Therefore, with minimal PP-pathway activity and all C
312 flowing via glycolysis, CO_2 was only released during the pyruvate dehydrogenase reaction (Fig. 2 (left); C_3
313 and C_4 lost as CO_2; all other C atoms are incorporated into the fatty acids; Table 2). However,
314 desaturation of palmitic acid (Olsson & Johansen, 2000) required an additional mol ATP per mol TPG
315 (0.032 mol glucose, producing ~0.19 mol CO_2 evenly from all six C atoms, and reducing CUE from 0.680
316 to 0.678). This had only a minor effect on the position-specific CO_2 production. The breakdown of
317 glucose to acetyl-CoA via the PP-pathway had a higher energy yield and most CO_2 was released from C_1
318 and C_4 (Fig. 2; Table 1, 2). The position-specific CO_2 production associated with PHB synthesis resembled
319 that of TPG (Table 2).
320 We did not model the synthesis of other storage compounds (starch, extracellular
321 polysaccharides, trehalose, other fatty acids, other polyhydroxyalkanoates). The metabolic pathways for
322 these compounds were closely related to those for glycogen, TPG or PHB, and would likely result in
323 similar CO_2 production patterns and CUE. The approach developed here can be used for the synthesis of

other hypothetical reserve compounds, at least as long as the details of the biosynthetic pathways are known.

3.3 Correlation between measured and modeled position-specific CO_2 production

The correlation between measured and modeled position-specific CO_2 production was low for CUE = 0, glycogen synthesis, and all cases where PP-pathway activity was low (Table 3). However, the modeled patterns of position-specific CO_2 production for maximal PP-pathway activity explained between 75-99% of the variance in the observed data. Although the modeled patterns of CUE = 0.3 and TPG and PHB synthesis (with maximal PP-pathway activity) exhibited high correlation coefficients (Table 3, Fig. 6), we found the best fit between observed and modeled position-specific CO_2 production for the hypothetical situation of balanced growth with a CUE = 0.6 and high PP-pathway activity (98-99% of variance explained; slope and intercept very close to the expected 1 : 1 line).

Combining low CUE (CUE = 0 or 0.3) with storage synthesis decreased the correspondence between modeled and observed position-specific CO_2 production. This is easiest understood by focusing on one C position, for example C_1. Assume CUE = 0 combined with sudden synthesis of TPG. In that case, CO_2 from C_1 during TPG synthesis assuming maximal PP-pathway activity (0.385) is combined with CO_2 production from C_1 for CUE = 0 (0.167). This will reduce the CO_2 production from C_1, and increase the difference between predicted and observed CO_2 production for this C atom (0.44 or 0.43 for ponderosa pine and piñon-juniper soil respectively). In fact, any combination of medium or low CUE and storage synthesis resulted in CO_2 production patterns that deviated more from observed patterns than those associated with storage compound synthesis alone.

4. DISCUSSION

Determining the position-specific CO_2 production from ^{13}C-labeled compounds is a straightforward and quick way to test biochemically explicit hypotheses for microbial processes, including storage compound synthesis, in microbial communities. In this study, we tested the mutually exclusive hypotheses that CUE of microbial substrate use is zero (substrate used for maintenance only - Hypothesis 1), CUE is low (important role for maintenance energy demand – Hypothesis 2), CUE is high because of "unbalanced" growth (storage compound production – Hypothesis 3), or CUE is high associated with balanced growth (Hypothesis 4). Based on the evidence presented, we conclude that the soil microbial community had a high CUE associated with balanced growth (Hypothesis 4).

The CUE observed is in the same range as found on average for soil ecosystems (~0.55) and higher than that in aquatic ecosystems (~0.3; Manzoni et al., 2012; Sinsabaugh et al., 2013). The two soils in this study exhibit similar patterns, suggesting that the metabolic processes in these soils are similar. Studies using a broad range of soils are required to determine whether this is a general pattern in soils. The results from this study demonstrate that observations of high CUE in earlier studies (e.g., Brant et al., 2006; Dijkstra et al., 2011a, b; Frey et al., 2013; van Groenigen et al., 2013; Hagerty et al., 2014; Hill et al., 2008; Nguyen & Guckert, 2001; Steinweg et al., 2008; Thiet et al., 2006; Tucker et al., 2013) do not necessarily represent storage compound synthesis as sometimes suggested (Blagodatskaya et al., 2014; Hill et al., 2008; Nguyen & Guckert, 2001; Reischke et al., 2014, 2015; Sinsabaugh et al., 2013), but may be related to balanced microbial growth.

4.1 High CUE: a consequence of glucose addition?

Although the results from this study exclude storage compound synthesis as an artefact, it does not eliminate other possible artefacts. The high CUE and balanced growth observed in this experiment may not be representative of microbial activity in unamended soil but a response to the glucose addition

371 used to measure CUE (Hypothesis 5). Several studies have suggested that glucose additions may alter
372 microbial growth and CUE, either increasing (van Groenigen et al., 2013; Sinsabaugh et al., 2013) or
373 decreasing it (van Groenigen et al., 2013; Russell, 2002). In the following, we will discuss the influence of
374 substrate addition on microbial growth and metabolism, specifically the effect of substrate
375 concentration and response time.

376 Substrate additions used to determine CUE range from 0.8 nmol glucose-C g^{-1} soil (Nguyen &
377 Guckert, 2001) to 61.5 µmol glucose-C g^{-1} soil (Thiet et al., 2006). The glucose applied in this experiment
378 is at the low end of this range (0.536 µmol glucose-C g^{-1} soil), and well within the range of
379 concentrations found in unamended soils (~1 nmol glucose-C g^{-1} soil - Fischer et al., 2007 - to 18 µmol g^{-1}
380 soil - Jones & Darrah, 1995). Yet, high CUE is found in this and other short-term experiments with even
381 lower glucose additions (0.8 nmol glucose-C g^{-1} soil, Nguyen & Guckert, 2001; 1.6 nmol glucose-C g^{-1} soil,
382 Hill et al., 2008). We conclude that there is no evidence to suggest that CUE is high because of
383 unnaturally high concentrations of substrate.

384 Anderson & Domsch (2010) and Reischke et al. (2014, 2015) find that glucose addition
385 stimulates microbial growth, but only after a lag-phase of 8 - 14 h and at high glucose concentrations (>
386 4.6 - 90 µmol glucose-C g^{-1} soil depending on soil type – Anderson & Domsch, 2010; > 41.5 µmol glucose-
387 C g^{-1} soil – Reischke et al., 2014; > 16 µmol glucose-C g^{-1} soil – Reischke et al., 2015). These
388 concentrations are higher than used in this experiment (0.536 µmol glucose-C g^{-1} soil), suggesting that
389 the glucose additions used in this experiment, and those by Nguyen & Guckert (2001) and Hill et al.
390 (2008), are too low and the incubation duration too short to induce microbial growth.

391 Furthermore, almost immediately after glucose addition, respiration increases, while microbial
392 growth rates remain unaffected (Reischke et al., 2014, 2015). These observations imply that CUE
393 decreases during the lag-phase in response to (a large) glucose addition. Similar declines in CUE are
394 found in pure culture studies where glucose addition rates exceed maximum growth rates or when

395 other nutrients than C limit growth (Russell 2007; Russell & Cook 1992). However, the CUE measured in
396 this experiment and by Nguyen & Guckert (2001) and Hill et al. (2008) are high, suggesting again that
397 substrate additions used did not affect microbial metabolism.

398 We conclude, based on existing studies on soil microbial community growth that the glucose
399 addition in this experiment is too low and incubation duration too short to induce microbial growth.
400 Furthermore, CUE was high and not low as expected during a lag-phase after glucose addition. Finally,
401 storage compound synthesis was ruled out as an artefact based on the observed position-specific CO_2
402 production patterns. Therefore, we tentatively conclude that the high CUE and balanced growth we
403 observed is representative of CUE in unamended soil.

404

405 *4.2 High CUE and maintenance energy requirements*

406 The high CUE observed seems in contradiction to the idea that soil is a C-limited environment
407 where most microbes are not growing or only grow slowly, and where maintenance energy demand
408 dominates substrate use (Blagodatskaya & Kuzyakov 2013; Reischke et al., 2015). Evidence of actively
409 dividing microbes is found by Rousk et al. (2011) and Reischke et al. (2014, 2015) in soil without glucose
410 additions, and in ^{18}O-H_2O stable isotope probing experiments (Schwartz, 2007). Blagodatskaya &
411 Kuzyakov (2013) conclude from extensive literature review that about 0.1-2% of the soil microbial cells
412 are actively growing and reproducing. This direct evidence of microbial growth in unamended soils
413 indicates that at least a portion of the microbial community has a high CUE and balanced growth.
414 Moreover, a low growth rate by itself, expected in C- and nutrient-limited soils, is not necessarily
415 associated with a low CUE. For example, a 10-fold reduction in growth rate (0.388 h^{-1} to 0.044 h^{-1}) in *E.*
416 *coli* pure cultures caused only a moderate reduction of CUE from 0.60 to 0.51 (Kayser et al., 2005).
417 Likewise, Lin et al. (2009) find no change in CUE for *Geobacillus* growth rates ranging between 0.053 h^{-1}
418 and 0.00078 h^{-1}.

A high CUE for the entire soil community is only possible if growing microbes with high CUE dominate microbial activity compared to microbes with low CUE. The community in soil is thought to consist of actively growing and dividing (0.1-2%), potentially growing (10-40%), and dormant microbes (remaining fraction; Blagodatskaya & Kuzyakov, 2013). To what degree the high CUE in a small, actively growing and dividing community is "diluted" by maintenance respiration of the inactive portion of the community may be calculated as follows. For simplicity, we assume that the active microbial fraction grows with a CUE near the highest values observed (CUE = 0.7), while the potentially active and dormant fractions conduct maintenance only (CUE = 0). Price & Sowers (2004) estimate ratios of metabolic rates of optimal-growth : maintenance : survival (dormancy) as $1 : 10^{-3} : 10^{-6}$. Applying these values to a community with 0.1-2% actively growing and dividing cells means that about 90-98% of substrate consumed is associated with actively growing microbes, and only 10-2% with potentially active or dormant microbes. A CUE of 0.7 for the actively growing community would then translate to a total community CUE of 0.64 (0.1% of community actively growing) or 0.69 (2% active). A similar argument is presented in Frey et al. (2001).

5. Conclusions

It is a well-established practice to use uniformly-labeled compounds to study microbial processes, including CUE. We show here that additional information is obtained by using position-specific ^{13}C-labeled compounds. This information can be used to test biochemically explicit hypotheses related to microbial physiology and biochemistry in soil microbial communities. We conclude that CUE in two soil microbial communities is high. This high CUE is not related to storage synthesis but to balanced growth, and appears to be unaffected by the small amount of glucose added.

The conclusion that the soil microbial community operates with a high CUE in soil environments has important and potential far-reaching consequences. It affects how we model microbial activity in

443 soils and think about the relative importance of maintenance processes. As a result, microbial death
444 (caused by viruses, grazing and predation) becomes more important as a key process in stabilizing
445 microbial population size and community composition (Hagerty et al., 2014), suggesting a possible top-
446 down control of microbial production by organisms at higher trophic levels. It also invites a rethinking of
447 the recalcitrant nature of soil organic matter and its suitability as a microbial substrate, and, as a
448 consequence, a rebalancing of the role of chemical vs physical protection in soil organic matter
449 stabilization (von Lützow et al., 2006). We conclude that the hypothesis of high CUE in undisturbed soil
450 remains viable and worthy of further testing.
451
452 **ACKNOWLEDGEMENTS**
453 This research is supported by NSF funding (DEB-1146449, DBI-0723250, and DBI-1126840). We thank
454 John Stark for the term 'balanced growth', and the anonymous reviewers for their constructive
455 comments.
456
457

458 **REFERENCES**

459 Allison, S.D., Wallenstein, M.D., Bradford, M.A., 2010. Soil-carbon response to warming dependent on
460 microbial physiology. Nature Geoscience 3, 336-340.

461 Alvarez, H.M., Steinbüchel, A., 2002. Triacylglycerols in prokaryotic microorganisms. Applied
462 Microbiology and Biotechnology 60, 367-376.

463 Amthor, J.S., 2000. The McCree – de Wit – Penning de Vries – Thornley respiration paradigms: 30 years
464 later. Annals of Botany 86, 1-20.

465 Anderson, T.-H., Domsch, K.H., 2010. Soil microbial biomass: the eco-physiological approach. Soil Biology
466 & Biochemistry 42, 2039-2043.

467 Billings, S.A., Ballantyne, F., 2013. How interactions between microbial resource demands, soil organic
468 matter stoichiometry, and substrate reactivity determine the direction and magnitude of soil
469 respiratory responses to warming. Global Change Biology 19, 90-102.

470 Blagodatskaya, E., Khomyakov, N., Myachina, O., Bogomolova, I., Blagodatsky, S., Kuzyakov, Y., 2014.
471 Microbial growth and carbon-use efficiency in the rhizosphere and root-free soil. PLoS ONE 9(4),
472 e93282. doi:10.1371/journal.pone.0093282.

473 Blagodatskaya, E., Kuzyakov, Y., 2013. Active microorganisms in soil: critical review of estimation criteria
474 and approaches. Soil Biology & Biochemistry 67, 192-211.

475 Bradford, M.A., 2013. Thermal adaptation of decomposer communities in warming soils. Frontiers in
476 Microbiology 4, 333 doi: 103389/fmicb201300333.

477 Brant, J.B., Sulzman, E.W., Myrold, D.D., 2006. Microbial community utilization of added carbon
478 substrates in response to long-term carbon input manipulation. Soil Biology & Biochemistry 38,
479 2219-2232.

480 Caspi, R., Altman, T., Billington, R., Dreher, K., Foerster, H., Fulcher, C.A., Holland, T.A., Keseler, I.M.,
481 Kothari, A., Kubo, A., Krummenacker, M., Latendresse, M., Mueller, L.A., Ong, Q., Paley, S.,

Subhraveti, P., Weaver, D.S., Weerasinghe, D., Zhang, P., Karp, P.D., 2014. The MetaCyc database of metabolic pathways and enzymes and the BioCyc collection of pathway/genome databases. Nucleic Acids Research 42, D459-D471.

Chapman, S.J., Gray, T.R.G., 1986. Importance of cryptic growth, yield factors and maintenance energy in models of microbial growth in soil. Soil Biology & Biochemistry 18: 1-4.

Coplen, T.B., 2011. Guidelines and recommended terms for expression of stable-isotope-ratio and gas-ratio measurement results. Rapid Communications in Mass Spectrometry 25, 2538-2560.

Dijkstra, P., Ishizu, A., Doucett, R., Hart, S.C., Schwartz, E., Menyailo, O.V., Hungate, B.A., 2006. ^{13}C and ^{15}N natural abundance of the soil microbial biomass. Soil Biology & Biochemistry 38, 3257-3266.

Dijkstra, P., Dalder, J., Selmants, P.C., Hart, S.C., Koch, G.W., Schwartz, E., Hungate, B.A., 2011a. Modeling soil metabolic processes using isotopologue pairs of position-specific ^{13}C-labeled glucose and pyruvate. Soil Biology & Biochemistry 43, 1848-1857.

Dijkstra, P., Thomas, S.C., Heinrich, P.L., Koch, G.W., Schwartz, E., Hungate, B.A., 2011b. Effect of temperature on metabolic activity of intact microbial communities: evidence for altered metabolic pathway activity but not for increased maintenance respiration and reduced carbon use efficiency. Soil Biology & Biochemistry 43, 2023-2031.

Fischer, H., Meyer, A., Fischer, K., Kuzyakov, Y., 2007. Carbohydrate and amino acid composition of dissolved organic matter leached from soil. Soil Biology & Biochemistry 39, 2926-2935.

Frey, S.D., Gupta, V., Elliott, E.T., Paustian, K., 2001. Protozoan grazing affects estimates of carbon utilization efficiency of the soil microbial community. Soil Biology & Biochemistry 33, 1759-1768.

Frey, S.D., Lee, J., Melillo, J.M., Six, J., 2013. The temperature response of soil microbial efficiency and its feedback to climate. Nature Climate Change 3, 395-398.

Gommers, P.J.F., van Schie, B.J., van Dijken, J.P., Kuenen, J.G., 1988. Biochemical limits to microbial-growth yields - an analysis of mixed substrate utilization. Biotechnology & Bioengineering 32, 86-94.

van Groenigen, K.J., Forristal, D., Jones, M., Smyth, N., Schwartz, E., Hungate, B., Dijkstra, P., 2013. Using metabolic tracer techniques to assess the impact of tillage and straw management on microbial carbon use efficiency in soil. Soil Biology & Biochemistry 66, 139-145.

Hagerty, S.B., van Groenigen, K.J., Allison, S.D., Hungate, B.A., Schwartz, E., Koch, G.W., Kolka, R.K., Dijkstra, P., 2014. Accelerated microbial turnover but constant growth efficiency with warming in soil. Nature Climate Change 4, 903-906.

Heijnen, J.J., van Dijken, J.P., 1992. In search of a thermodynamic description of biomass yields for the chemotropic growth of microorganisms – response. Biotechnology & Bioengineering 42, 1127-1130.

Heijnen, J.J., 2010. Impact of thermodynamic principles in systems biology. In: Biosystems Engineering II: Linking Cellular Networks and Bioprocesses. Volume 121: Advances in Biochemical Engineering-Biotechnology (eds. C. Wittmann, R. Krull). Pp. 139-162.

Hill, P.W., Farrar, J.F., Jones, D.L., 2008. Decoupling of microbial glucose uptake and mineralization in soil. Soil Biology & Biochemistry 40, 616-624.

Hobbie, J.E., Hobbie, E.A., 2013. Microbes in nature are limited by carbon and energy: the starving-survival lifestyle in soil and consequences for estimating microbial rates. Frontiers in Microbiology 4, 324 doi: 10.3389/fmicb.2013.00324.

Jones, D.L., Darrah, P.R., 1995. Influx and efflux of organic acids across the soil root interface of *Zea mays* L. and its implications in rhizosphere C flow. Plant & Soil 173, 103-109.

de Kok, S., Kozak, B.U., Pronk, J.T., van Maris, A.J.A., 2012. Energy coupling in *Saccharomyces cerevisiae*: selected opportunities for metabolic engineering. FEMS Yeast Research 12, 387-397.

528 Kosa, M., Ragauskas, A.J., 2011. Lipids from heterotrophic microbes: advances in metabolism research.
529 Trends in Biotechnology 29, 53- 61, doi:10.1016/j.tibtech.2010.11.002
530 Li, J.W., Wang, G.S., Allison, S.D., Mayes, M.A., Luo, Y.Q., 2014. Soil carbon sensitivity to temperature
531 and carbon use efficiency compared across microbial-ecosystem models of varying complexity.
532 Biogeochemistry 119, 67-84, doi:101007/s10533-013-9948-8.
533 Lu, J., Tappel, R.C., Nomura, C.T., 2009. Mini-Review: Biosynthesis of poly(hydroxyalkanoates). Polymer
534 Reviews 49, 226-248.
535 Manzoni, S., Taylor, P., Richter, A., Porporato, A., Ågren, G.I., 2012. Environmental and stoichiometric
536 controls on microbial carbon-use efficiency in soils. New Phytologist 196, 79-91.
537 Nguyen, C., Guckert, A., 2001. Short-term utilization of ^{14}C-[U]glucose by soil microorganisms in relation
538 to carbon availability. Soil Biology & Biochemistry 33, 53-60.
539 Olsson, P.A., Johansen, A., 2000. Lipid and fatty acid composition of hyphae and spores of arbuscular
540 mycorrhizal fungi at different growth stages. Mycological Research 4, 429-434.
541 Price, P.B., Sowers, T., 2004. Temperature dependence of metabolic rates for microbial growth,
542 maintenance, and survival. Proceedings of the National Academy of Science 101, 4631-4636.
543 Reischke, S., Kumar, M.G.K., Bååth, E., 2015. Threshold concentration of glucose for bacterial growth in
544 soil. Soil Biology & Biochemistry 70, 88-95.
545 Reischke, S., Rousk, J., Bååth, E., 2014. The effects of glucose loading rates on bacterial and fungal
546 growth in soil. Soil Biology & Biochemistry 70, 88-95.
547 Roels, J.A., 1980. Application of macroscopic principles to microbial-metabolism. Biotechnology &
548 Bioengineering 22, 2457-2514.
549 Russell, J.B., 2007. The energy spilling reactions of bacteria and other organisms. Journal of Molecular
550 Microbiology and Biotechnology 13, 1-11.

551 Russell, J.B., Cook, G.M., 1995. Energetics of bacterial growth: balance of anabolic and catabolic
552 reactions. Microbiological Reviews 59, 48-62.
553 Schwartz, E., 2007. Characterization of growing microorganisms in soil by stable isotope probing with
554 $H_2{}^{18}O$. Applied and Environmental Microbiology 73, 2541-2546.
555 Sinsabaugh, R.L., Manzoni, S., Moorhead, D.L., Richter, A., 2013. Carbon use efficiency of microbial
556 communities: stoichiometry, methodology and modelling. Ecology Letters 16, 930-939.
557 Steinweg, J.M., Plante, A.F., Conant, R.T., Paul, E.A., Tanaka, D.L., 2008. Patterns of substrate utilization
558 during long-term incubations at different temperatures. Soil Biology & Biochemistry 40, 2722-
559 2728.
560 Thiet, R.K., Frey, S.D., Six, J., 2006. Do growth yield efficiencies differ between soil microbial
561 communities differing in fungal:bacterial ratios? Reality check and methodological issues. Soil
562 Biology & Biochemistry 38, 837-844.
563 Tucker, C.L., Bell, J., Pendall, E., Ogle, K., 2013. Does declining carbon-use efficiency explain thermal
564 acclimation of soil respiration with warming? Global Change Biology 19, 252-263.
565 von Lützow, M., Kögel-Knabner, I., Ekschmitt, K., Matzner, E., Guggenberger, G., Marschner, B., Flessa,
566 H., 2006. Stabilization of organic matter in temperate soils: mechanisms and their relevance
567 under different soil conditions – a review. European Journal of Soil Science 57, 426-445.
568 Wieder, W.R., Bonan, G.B., Allison, S.D., 2013. Global soil carbon projections are improved by modelling
569 microbial processes. Nature Climate Change 3, 909-912.
570 Wilson, W.A., Roach, P.J., Montero, M., Baroja-Fernández, E., Muñoz, F.J., Eydallin, G., Viale, A.M.,
571 Pozueta-Romero, J., 2010. Regulation of glycogen metabolism in yeast and bacteria. FEMS
572 Microbiology Review 34, 952-985.

573 Wilson-O'Brien, A.L., Patron, N., Rogers, S., 2010. Evolutionary ancestry and novel functions of the
574 mammalian glucose transporter (GLUT) family. BMC Evolutionary Biology 10: 152, doi:
575 10.1186/1471-2148-10-152.
576 Xiao, J.H., van Briesen, J.M., 2006. Expanded thermodynamic model for microbial true yield prediction.
577 Biotechnology & Bioengineering 93, 110-121.
578 Ziegler, S.E., White, P.M., Wolf, D.C., Thoma, G.J., 2005. Tracking the fate and recycling of ^{13}C-labeled
579 glucose in soil. Soil Science 170, 767-778.
580

581 TITLES AND LEGENDS TO FIGURES

582 Fig. 1. Model and mass balance equations for calculation of fluxes through the central C metabolic
583 network (after Dijkstra et al., 2011a). Relative to a previous version, pentose phosphate pathway and
584 TCA cycle representations are simplified by combining several reactions. These alterations do not
585 change model outcomes. Flux rates (reactions r2-r11 and biosynthesis reactions br1-br8) are normalized
586 to glucose uptake rate (r1, set at 100) on a molar basis. Abbreviations: G6P, glucose-6P; F1,6P, fructose-
587 1,6P2; GAP, glyceraldehyde-P; PYR, pyruvate; ACCO, acetyl-CoA; ICIT, isocitrate; αKG, α-ketoglutarate;
588 OAA, oxaloacetate; RU5P, ribulose-5P; S7P, sedoheptulose-7P; E4P, erythrose-4P.

589

590 Fig. 2. Diagram of glucose breakdown via glycolysis (left) and PP-pathway (right) to acetyl-CoA and CO_2
591 (red circles). Number in circles refer to the C-atom position in the original glucose molecule.

592

593 Fig. 3. Rates of CO_2 production for six glucose isotopomers in ponderosa pine soil (A; means and S.E.)
594 and position-specific CO_2 production (relative to U-^{13}C labeled glucose; B; means and 95% confidence
595 interval) for ponderosa pine and piñon-juniper soil. Letters indicate significant differences between C
596 positions for ponderosa pine (upper case) and piñon-juniper (lower case) soil.

597

598 Fig. 4. Modeled position-specific CO_2 production (relative to U-^{13}C labeled glucose) for CUE = 0, 0.3, and
599 0.6 for minimal (A) and maximal (B) pentose phosphate pathway activity.

600

601 Fig. 5. Modeled position-specific CO_2 production (relative to U-^{13}C labeled glucose) for CUE = 0.6 for
602 minimal (A) and maximal (B) pentose phosphate pathway activity for proportional precursor demand
603 characteristic for Gram-negative bacteria, Gram-positive bacteria, and fungi.

604

Fig. 6. Modeled versus observed position-specific CO_2 production (relative to U-^{13}C labeled glucose; means and 95% confidence interval) for ponderosa pine (red squares) and piñon-juniper soil (green circles) for modeled balanced growth with CUE = 0.6 (A), CUE = 0.3 (B), and tri-palmitoyl glycerol synthesis (C) with maximal pentose phosphate pathway activity. Dashed lines are the expected 1:1 relationships. Information on regression statistics is available in Table 3.

Table

Table 1: Carbon Use Efficiency of glycogen, tri-palmitoyl-glycerol, and polyhydroxybutyrate synthesis assuming minimal and maximal pentose phosphate pathway activity calculated from stoichiometry of synthesis reactions (eq. 3-6).

	CUE
Minimal pentose phosphate pathway	
Glycogen	0.90
Tri-palmitoyl-glycerol	0.68
Polyhydroxybutyrate	0.67
Maximal pentose phosphate pathway	
Glycogen	0.90
Tri-palmitoyl-glycerol	0.57
Polyhydroxybutyrate	0.56

Table

Table 2: Predicted CO_2 production patterns associated with glycogen, tri-palmitoyl-glycerol and polyhydroxybutyrate synthesis assuming minimal and maximal pentose phosphate pathway activity. $^{\$}$ and ^{A} indicate significant differences with observed position-specific CO_2 production for ponderosa pine and piñon-juniper soil respectively.

	C_1	C_2	C_3	C_4	C_5	C_6
Minimal pentose phosphate pathway						
Glycogen	$0.167^{\$A}$	$0.167^{\$A}$	$0.167^{\$A}$	$0.167^{\$A}$	$0.167^{\$A}$	$0.167^{\$A}$
Tri-palmitoyl-glycerol	$0.000^{\$A}$	$0.000^{\$A}$	$0.500^{\$A}$	$0.500^{\$A}$	$0.000^{\$A}$	$0.000^{\$A}$
Polyhydroxybutyrate	$0.000^{\$A}$	$0.000^{\$A}$	$0.500^{\$A}$	$0.500^{\$A}$	$0.000^{\$A}$	$0.000^{\$A}$
Maximal pentose phosphate pathway						
Glycogen	$0.167^{\$A}$	$0.167^{\$A}$	$0.167^{\$A}$	$0.167^{\$A}$	$0.167^{\$A}$	$0.167^{\$A}$
Tri-palmitoyl-glycerol	0.385	0.128	$0.128^{\$}$	$0.359^{\$A}$	$0.000^{\$A}$	$0.000^{\$A}$
Polyhydroxybutyrate	$0.375^{\$}$	$0.125^{\$A}$	$0.125^{\$}$	$0.375^{\$A}$	$0.000^{\$A}$	$0.000^{\$A}$

Table

Table 3. Correlation of observed position-specific CO_2 production pattern for ponderosa pine (first number) and pinon-juniper soil (second number) with modeled CO_2 production patterns for balanced growth (CUE = 0, CUE = 0.3. CUE = 0.6), and glycogen, tri-palmitoyl-glycerol, and polyhydroxybutyrate synthesis with minimal or maximal pentose phosphate pathway activity.

	R^2	Slope	Intercept
Minimal pentose phosphate pathway			
CUE = 0	0.00 / 0.00	0.00 / 0.00	0.167 / 0.167
CUE = 0.3	0.00 / 0.01	-0.01 / 0.02	0.168 / 0.164
CUE = 0.6	0.00 / 0.04	0.03 / 0.12	0.162 / 0.146
Glycogen	0.00 / 0.00	0.00 / 0.00	0.167 / 0.167
Tri-palmitoyl-glycerol	0.00 / 0.01	-0.10 / 0.21	0.183 / 0.131
Polyhydroxybutyrate	0.00 / 0.01	-0.10 / 0.21	0.183 / 0.131
Maximal pentose phosphate pathway			
CUE = 0	0.00 / 0.00	0.00 / 0.00	0.167 / 0.167
CUE = 0.3	0.91 / 0.95	0.27 / 0.30	0.121 / 0.115
CUE = 0.6	0.98 / 0.99	0.92 / 1.03	0.010 / -0.007
Glycogen	0.00 / 0.00	0.00 / 0.00	0.167/ 0.167
Tri-palmitoyl-glycerol	0.78 / 0.90	1.04 / 1.23	-0.010 / -0.042
Polyhydroxybutyrate	0.75 / 0.88	1.02 / 1.23	-0.007 / -0.041

Figure

Fig. 1

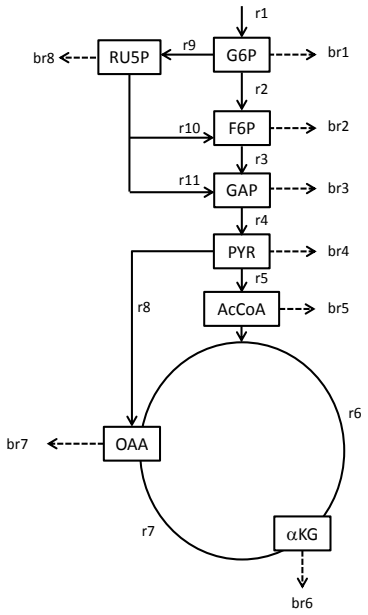

Equations

1- G6P: r1=r9+r2+br1
2- F6P: r2+r10=r3+br2
3- GAP: r3+r11=r4+br3
4- PYR: r4=r5+r8+br4
5- AcCoA: r5=r6+br5
6- αKG: r6=r7+br6
7- OAA: r7+r8=r6+br7
8- RU5P: r9=r10+r11+br8

Figure

Fig. 2.

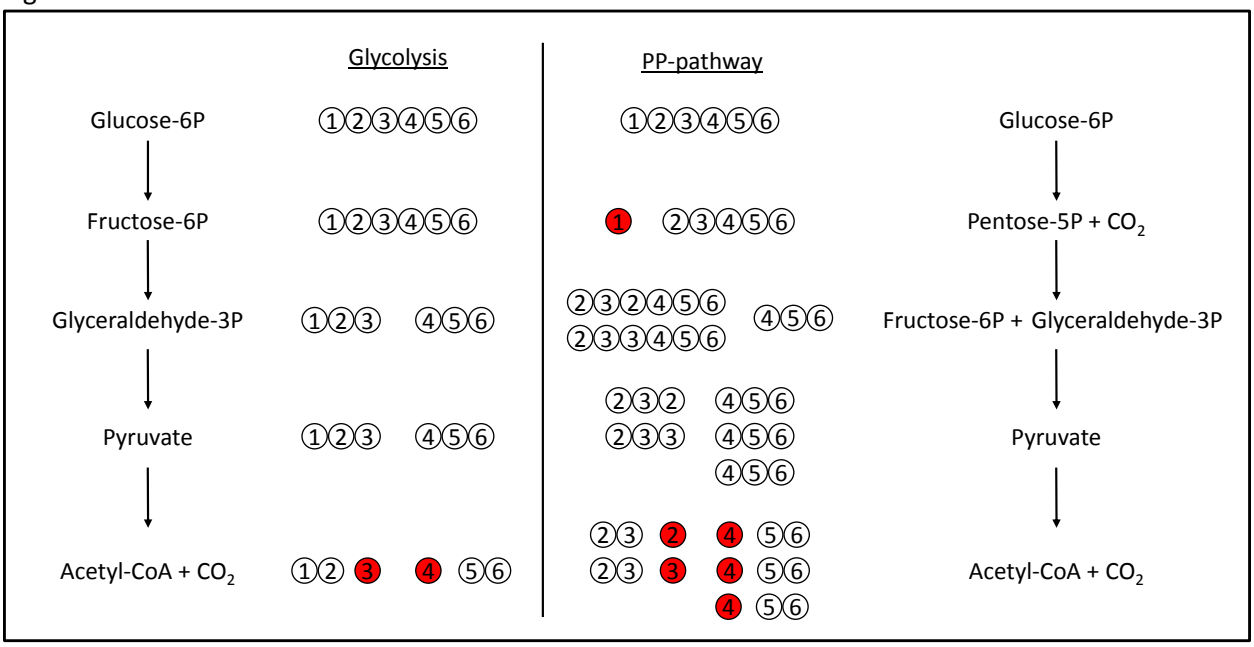
Glycolysis
PP-pathway
Glucose-6P
Fructose-6P
Glyceraldehyde-3P
Pyruvate
Acetyl-CoA + CO2
Glucose-6P
Pentose-5P + CO2
Fructose-6P + Glyceraldehyde-3P
Pyruvate
Acetyl-CoA + CO2

Figure

Fig. 3

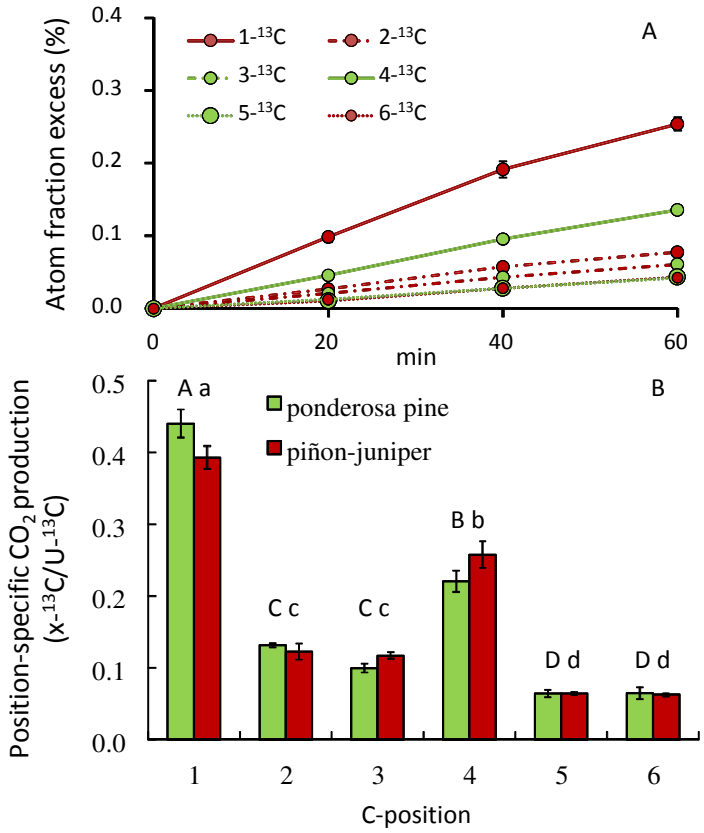
A
1-13C
2-13C
3-13C
4-13C
5-13C
6-13C
Atom fraction excess (%)
0.4
0.3
0.2
0.1
0.0
0
20
40
60
min
B
ponderosa pine
piñon-juniper
Position-specific CO2 production
(x-13C/U-13C)
A a
B b
C c
C c
D d
D d
0.5
0.4
0.3
0.2
0.1
0.0
1
2
3
4
5
6
C-position

Figure

Fig. 4

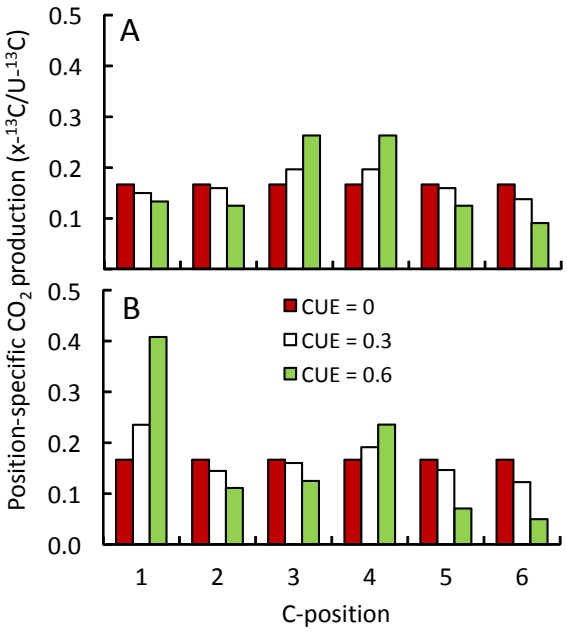
A
B
CUE = 0
CUE = 0.3
CUE = 0.6
Position-specific CO2 production (x-13C/U-13C)
C-position
0.0
0.1
0.2
0.3
0.4
0.5
1
2
3
4
5
6

Figure

Fig. 5.

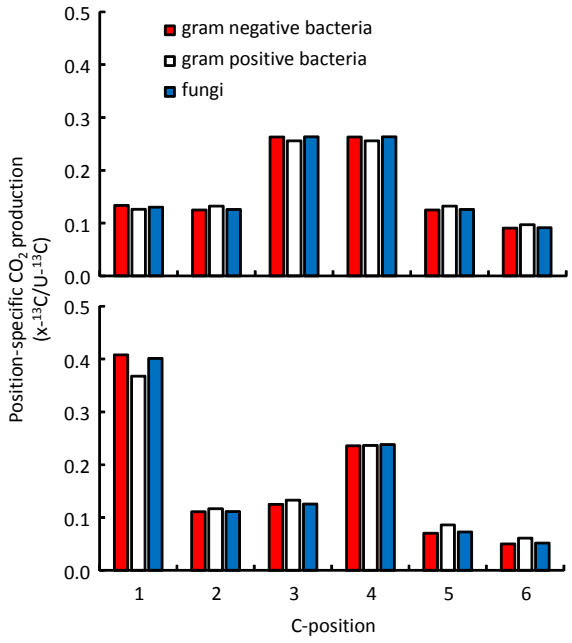
gram negative bacteria
gram positive bacteria
fungi
Position-specific CO_2 production ($x^{-13}C/U^{-13}C$)
0.0
0.1
0.2
0.3
0.4
0.5
1
2
3
4
5
6
C-position

Figure

Fig. 6.

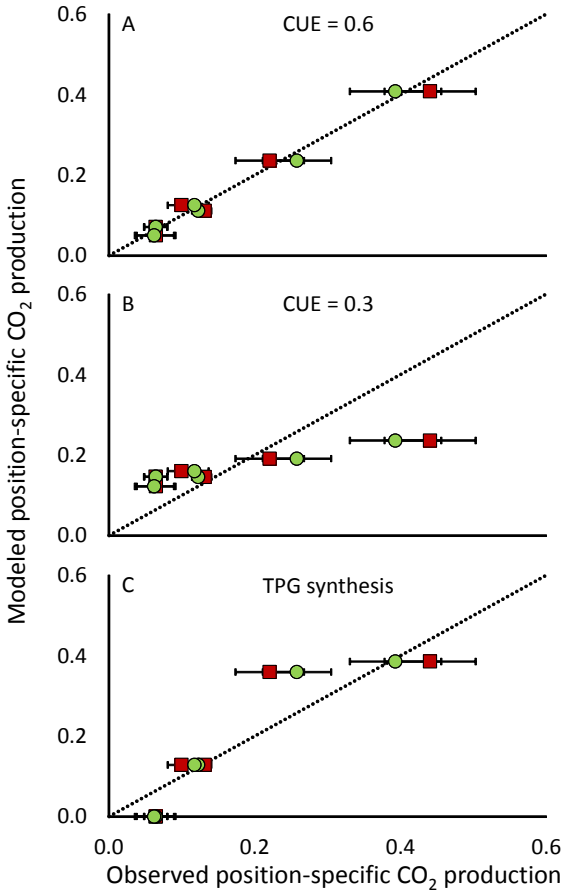
A
CUE = 0.6
B
CUE = 0.3
C
TPG synthesis
0.0
0.2
0.4
0.6
Modeled position-specific CO_2 production
Observed position-specific CO_2 production